

# Influence of water content on dynamic mechanical properties of coal

Helong Gu<sup>1</sup>, Ming Tao<sup>\*1</sup>, Jingxiao Wang<sup>1</sup>, Haibo Jiang<sup>1,2</sup>, Qiyue Li<sup>1</sup> and Wen Wang<sup>3</sup>

<sup>1</sup>School of Resources and Safety Engineering, Central South University, Changsha, Hunan, 410083, People's Republic of China

<sup>2</sup>Safety Engineering Institute, Hunan Vocational Institute of Safety Technology, Changsha, Henan, 410151, People's Republic of China

<sup>3</sup>School of Energy Science and Engineering, Henan Polytechnic University, Jiaozuo, Henan, 454003, People's Republic of China

(Received December 5, 2017, Revised March 15, 2018, Accepted March 29, 2018)

**Abstract.** Water affects the mechanical properties of coal and stress wave propagation. To comprehensively investigate the effect of water content on the properties of coal, laboratory tests including X-Ray Diffraction (XRD) analysis, P-wave test, S-wave test, static and dynamic compression test with different water contents were conducted. The compressive strength, elastic modulus and failure strain and their mechanism of coal specimen under coupled static-dynamic load with the increased water content were observed. Meanwhile, energy transmission and dissipation characteristics of a stress wave in coal specimens with different water contents under dynamic load and its relation with the failure features, such as fragmentation and fractal dimension, of coal was analyzed. Furthermore, the dynamic interpretation of water infusion to prevent coal burst based on water infusion model of coal seam roadway was provided.

**Keywords:** coal; water content; dynamic mechanical properties; stress wave propagation; failure features

## 1. Introduction

Water content as an important parameter influencing the mechanical properties of coal and plays a key role in the effect of coal seam water infusion (Cheng *et al.* 2012). The physical and static mechanical properties of coals with different water contents have been extensively investigated in previous studies, but, the dynamic mechanical properties of coal with different water contents have rarely been studied. The dynamic mechanical properties of coal are special importance in understanding the mechanism of coal seam water infusion preventing coal burst from the dynamic perspectives and guiding the engineering practice of coal seam water infusion. Therefore, it is necessary to continue the study of the dynamic mechanical properties of coal with different water contents.

To prevent and control dynamic disasters, water infusion is commonly adopted to improve rock mass properties, alleviate high stress concentration, and reduce the accumulation level of elastic energy. The study about the effect of water content on coal under different water contents mainly focus on static properties (Yao *et al.* 2015). However, when a dynamic disturbance occurs in an underground blasting or other the mining process, the mechanical properties of coal with certain water content are inevitably affected by dynamic loading. Zhao *et al.* (2016) tested the dynamic tensile strength of rock under dry and saturated conditions, obtaining that compared with dry coal specimens saturated ones have higher indirect tensile strength. To further explore the dynamic characteristics of

rock under different water contents, Zhou *et al.* (2011, 2016) carried out a series of dynamic compressive experiments on rock with different water contents, and a significant amount of information on the dynamic mechanical properties of rock under conditions of different water contents were achieved. Ogata (2004) tested the porous rock with different water saturation levels, getting that dynamic tensile strength decreased with increased water saturation level. To investigate the dynamic properties of coal under different water contents, Zheng *et al.* (1991) tested two groups of coal specimen of two porosity conditions with different water contents and indicated that with the increase of water content, the dynamic modulus of coal with large porosity enhance, and the coal with small porosity shows the opposite effect. The previous studies involves the dynamic mechanical features of coal under different water contents, the other important mechanical properties such as stress wave propagation characteristics, dynamic strength and its mechanism with different water contents were not involved.

Additionally, the coal seam disturbed during the mining process, the stress condition of coal in the state of a coupled static-dynamic loads. Meanwhile, the mechanical properties of coal with different water contents under coupled static-dynamic loads is better reflect the stress state of a coal seam. Therefore, the mechanism of the variation of dynamic mechanical properties of coal with different water contents is highly necessary to the understanding of the functionary mechanism of water content on the dynamic mechanical properties of coal caused by the dynamic load in a water-rich area. Coal seam dynamic disaster is a process of energy propagation and dissipation, and the failure processes of coal are accompanied by the absorption and dissipation of energy (Gaziev 2010). Many factors such as the strain rate (Liu *et al.* 2009), slenderness ratio (Li *et al.* 2014), incident

\*Corresponding author, Professor  
E-mail: [mingtao@csu.edu.cn](mailto:mingtao@csu.edu.cn)

energy (Hong *et al.* 2009), and fragmentation (Whittles *et al.* 2006) have been verified. However, the effect of water content as an important index of coal quality on the energy dissipation of coal has not been involved. In addition, water content has an important influence on the wave impedance by affecting the density of coal specimens, and the propagation velocity of the P-wave, which has a significant influence on the propagation of stress wave, are changed inevitably. However, the effect of the water content on stress wave propagation in coal is still unclear. Thus, it is necessary to systematically and comprehensively study the effects of water content on the physical and stress wave propagation properties of coal specimens, which will provide a theoretical basis for understanding the effect of water content on the energy propagation and dissipation of coal during failure process under dynamic load.

This study attempts to reveal the influence and its mechanism of water content on the stress wave propagation and the mechanical properties of coal under static load and coupled static-dynamic loads. The RMT-150 rock mechanics testing machine and the Split Hopkinson Pressure Bar apparatus (SHPB) were applied to test a series of coal specimens with different water contents at 25°C. The deformation, strength and elastic modulus properties of coal with different water contents under dynamic load and static load were investigated. The relations among energy density, fragmentation and water content, and the effect of water content on the propagation of stress wave energy in coal were revealed.

## 2. Specimen preparation and water treated

The coal used in this study was collected from the Yima mine area in Henan, China, where the buried depth of coal seam has reached more than 1000 meters. Dozens of coal bursts in roadway have been witnessed in this area and frequently caused the collapse and serious deformation of the roadway, as shown in Fig. 1. Currently, coal seam water infusion in the area is one of the most important methods for coal burst prevention. Therefore, it is urgent need to investigate the influence of water content on the dynamic mechanical properties of coal. The mineral composition of the coal was determined by X-ray diffraction (XRD), and the results are shown in Table 1.

Specimens were extracted from one block of coal and manufactured with high geometrical integrity and petrographical uniformity in accordance with the specifications of the International Society of Rock Mechanics (ISRM) (ISRM *et al.* 1978, Zhou *et al.* 2011). All specimens were cut into 50-mm diameter cylinders and polished to achieve a surface roughness less than 0.02 mm, and the end surfaces were perpendicular to the cylinder axis within 0.001 radians, as shown in Fig. 2. The bulk volume was calculated based on the diameter and height, as measured using a vernier calliper with an accuracy of 0.02 mm, and the mass was obtained using an electronic balance with an accuracy of 0.01 g. The bulk volume was calculated based on the diameter and height, as measured using a vernier calliper with an accuracy of 0.02 mm, and the mass was obtained using an electronic balance with an accuracy of 0.01 g.



Fig. 1 Coal sample collection site information

Table 1 Mineral composition of coal specimen

Mineral composition	Chemical formula	Content (%)
Kaolinite	$Al_4[Si_4O_{10}](OH)_8$	33.2
Illite	$K_{0.9}Al_{2.9}Si_{3.1}O_{10}(OH)_2$	30.2
Chlorite	$(Mg, Fe)_5(Al, Fe)_2Si_3O_{10}(OH)_8$	2.7
Montmorillonite	$(Na, Ca)_{0.33}(Al, Mg)_2[Si_4O_{10}](OH)_2$	17.7
Quartz	$SiO_2$	2.8
Potash feldspar	$KAlSi_3O_8$	3.2
Calcite	$CaCO_3$	1.7
Dolomite	$CaMg(CO_3)_2$	4.1
Hematite	$Fe_2O_3$	4.9

Randomly, the coal specimens were divided into two groups, i.e., csa and csd, which were used in the static compressive tests and the dynamic compressive tests, respectively. The length/diameter ratio of the specimens was 0.6 and they were stored in a laboratory with excellent ventilation for one month to ensure that they were dry before the tests.

A dry specimen was inundated for 2 hours (h) in a tank filled with purified water, and then it was taken out and weighed. The operations were repeated every 2h until the weight of the specimen remained unchanged, then the specimen was considered saturated. The laboratory temperature was constant at 25°C in the entire specimen preparation process, as shown in Fig. 2. During the test, the static and coupled static-dynamic tests proceeded independently. The weight increase was used to determine the water content of the specimens at the different soaking times as follows

$$w = \frac{m_t - m_d}{m_d} \times 100\% \quad (1)$$

where  $w$  is the water content of the specimen,  $m_t$  is the weight of the specimen that soaking in water for a period of time, and  $m_d$  is the dry weight of the specimen.

Table 2 shows the parameters of the specimens with different water contents. The dry coal specimens reached a saturated state after approximately 8h and the maximum water contents of the two groups (csa and csd) were 5.13% and 4.9%. Then, the specimens with different water contents were transmitted by ultrasonic (1 MHz frequency) compression (P) and shear (S) waves along the direction of its length, when the pre-stress was maintained constant. The velocity of the wave was calculated based on the received wave forms and the propagation time in the specimen, and used to determine the dynamic mechanical properties.

Figs. 3 and 4 show the variations of P-wave and S-wave velocities as functions of water content. Fig. 3 indicates that

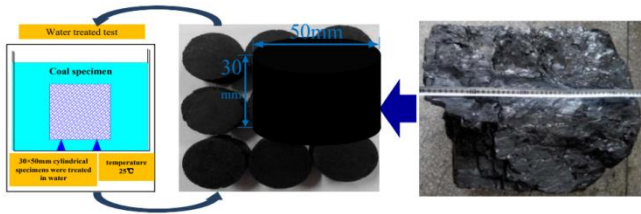


Fig. 2 Manufacturing process of coal specimen with different water contents

Table 2 Specimen parameters in static compressive tests

Specimen no.	Density(kg.m <sup>-3</sup> )		Water content (%)	Strength (MPa)	Elasticmodulus (GPa)	Failure strain
	Dried	Water treated				
csa1-1	1.2785	--	0	33.42	1.358	0.0181
csa1-2	1.2726	--	0	32.55	2.342	0.0154
csa1-3	1.2653	--	0	30.26	1.637	0.0129
csa2-2	1.2776	1.296	1.46	28.65	1.038	0.0161
csa2-1	1.2661	1.285	1.48	23.57	1.373	0.0191
csa2-3	1.2788	1.298	1.52	25.21	0.990	0.0182
csa3-1	1.2585	1.297	3.12	22.81	1.240	0.0154
csa3-2	1.2568	1.295	3.05	20.45	0.965	0.0156
csa3-3	1.2675	1.305	3.02	20.92	0.714	0.0227
csa4-1	1.2792	1.339	4.73	19.91	0.462	0.0152
csa4-2	1.2485	1.308	4.79	16.6	0.566	0.0216
csa4-3	1.2554	1.319	5.13	18.8	0.972	0.0257

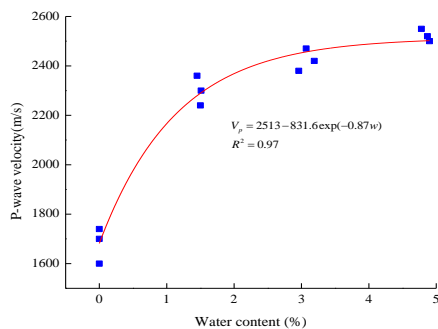


Fig. 3 Relation of P-wave velocity and water content

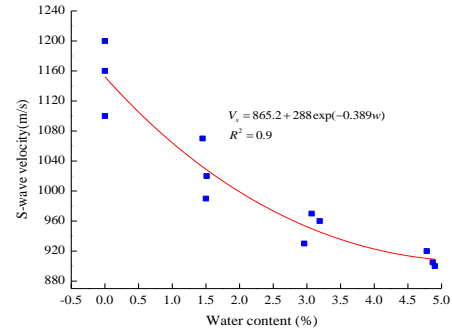


Fig. 4 Relation of S-wave velocity and water content

as the saturation level increases, the P-wave velocity increases until the water content reaches 2%, then, the P-wave velocity increases slightly and finally remain at approximately 2400 m/s. In the water absorption process of coal specimens, water entering the fractures and pores will enhance P-wave transmissivity because of its higher density. Meanwhile, the soluble mineral dissolve and particles density of coal decline because of gradually enhanced water-coal interaction and dilution effect. It makes the density even more uniform in the coal specimen leading to the P-wave velocity of the coal specimen tends to steady. Fig. 4 indicates a decrease in the S-wave velocity as the water content increase. There are large numbers of pores and fractures in coal and the angle between these fractures and the vibration direction of S-wave are different. When the angle between the fracture and the direction of the S-wave is small, the vibration propagates in fracture through the fillings in the fracture or the contact part of the rough fracture wall. When the water enter into the fracture, the water tend to dissolve the fillings and drive the fracture expansion, which will reduce the contact area in fractures and enhance the damping effect on the vibration of S-wave. Therefore, the more fracture development, especially the fracture with small angle in the direction of the vibration of the particle, the more remarkable of S-wave velocity decreases with the increased water content. The relations of P-wave velocity  $V_p$ , S-wave velocity  $V_s$  and water content can be described by the following equations

$$V_p = 2513 - 831.6\exp(-0.87w) (R^2 = 0.97) \quad (2)$$

$$V_s = 865.2 + 288\exp(-0.389w) (R^2 = 0.9) \quad (3)$$

### 3. Static mechanical properties of coal with different water contents

Coal seam water infusion can reduce the strength in the stress concentration region of the surrounding rock and promote the transfer of stress to the deep part of the surrounding rock. To reveal the static mechanical properties of coal with different water contents, static load experiments were carried out by RMT-150, and the static compressive stress-strain curves of specimens with different water contents are shown in Fig. 5, where  $w_a$  represented the average water content. In compressive time-consuming

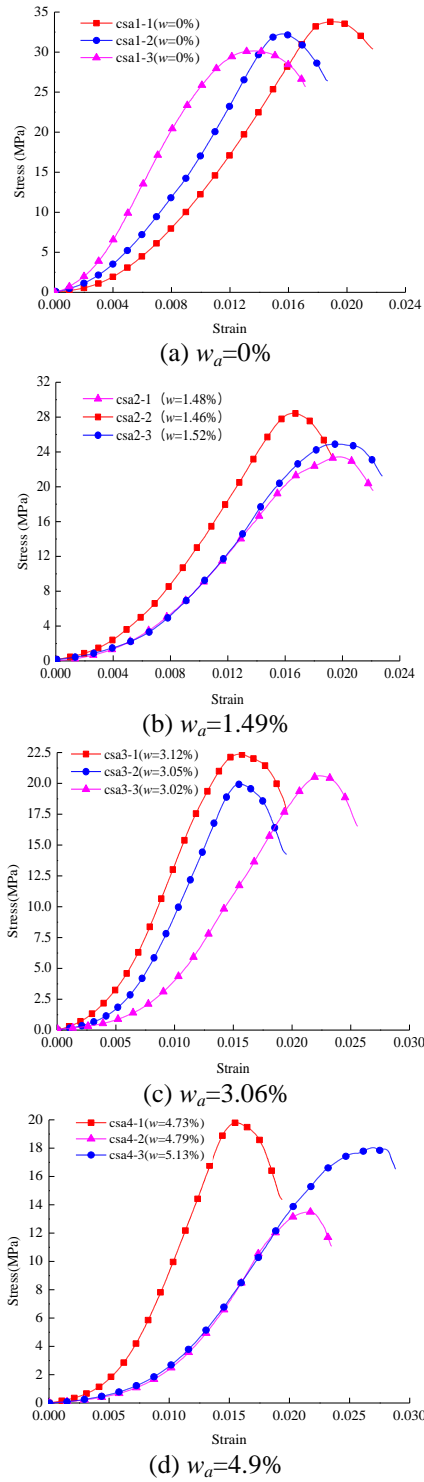


Fig. 5 Static stress-strain curves of coal specimens with different water contents

testing procedures (Shen *et al.* 2014), there is an initial compaction stage when the existing micro-fractures and pores are squeezed to close. Then, the stress-strain curves are almost linear until the peak strength is reached. The stress-strain curve, strength and modulus of coal specimens are different to some extent with approximately the same water content, which reflects the discreteness of coal. These mechanical parameters gradually decline with the increase

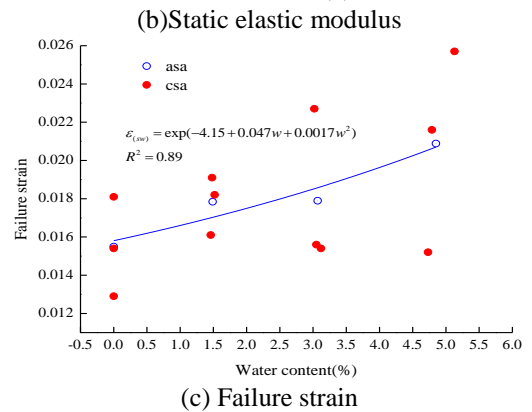
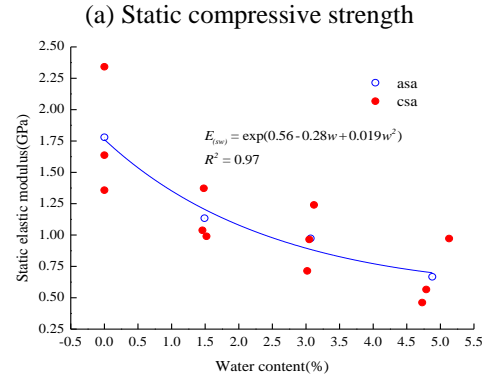
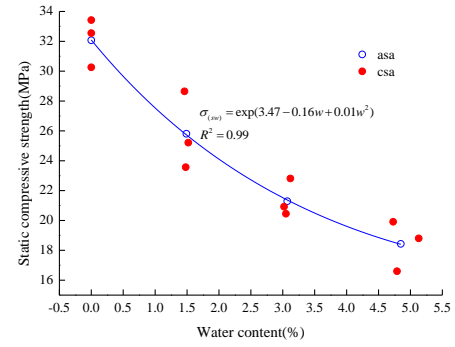


Fig. 6 Relation between static mechanical parameters and water content (\*asa represents the mean value of static mechanical parameters of specimens with the similar water content)

of water content, which indicate that water content can reduce the carrying and anti-deformation capacity (Shen *et al.* 2012). And the parameters of coal specimens detailed in Table 2. Meanwhile, the brittleness of coal decreases and ductility increases with the increased water content. The relations among static compressive strength, failure strain, static elastic modulus and water content can be described as the follow exponential equation

$$W = \exp(a + bw + cw^2) \quad (4)$$

where  $W$  represent static compressive strength, failure strain or static elastic modulus;  $w$  is water content;  $a$ ,  $b$  and  $c$  are constants.

Fig. 6 shows that when specimens change from a dry to a saturated state, their average static compressive strengths and elastic modulus decreased from 32.2 MPa and 3.2 GPa to 19.1 MPa and 1.6 GPa, with the reductions of approximately 40.6% and 50%, respectively. The average

Table 3 The relation of static and dynamic properties of coal with different water contents

Properties	Category	Relation Equations
Strength	Dynamic	$\sigma_{(dw)} = \exp(3.65 - 0.12w + 0.0025w^2)(R^2 = 0.99)$
	Static	$\sigma_{(sw)} = \exp(3.46 - 0.16w + 0.01w^2)(R^2 = 0.99)$
Elastic modulus	Dynamic	$E_{(dw)} = \exp(2.98 - 2.1w + 0.013w^2)(R^2 = 0.95)$
	Static	$E_{(sw)} = \exp(0.56 - 0.28w + 0.019w^2)(R^2 = 0.97)$
Failurestrain	Dynamic	$\varepsilon_{(dw)} = \exp(-4.93 - 0.1w - 0.0034w^2)(R^2 = 0.9)$
	Static	$\varepsilon_{(sw)} = \exp(-4.15 + 0.047w + 0.0017w^2)(R^2 = 0.89)$

failure strain increase from 0.0155 to 0.021, with the enhancements of approximately 35.4%, which indicates that water content can not only weaken the stress concentration of the coal seam, but also enhance the deformation capacity.

With the increase of water content, these properties of coal specimens change exponentially, as shown in Table 3. The failure state for coal specimens with different water contents is also different. Fig. 10(a) shows that the failure lumpiness of coal specimen obviously decrease with the increased water content, which manifest that water content can reduce the energy required for the destruction of a coal specimen.

#### 4. Influence of water content on dynamic mechanical properties of coal

The modified SHPB apparatus was applied to conduct the dynamic mechanical properties of coal, which can realize coupled static-dynamic loads (Li *et al.* 2008), as shown in Fig. 7. The apparatus are detailed described in the previous study (Tao *et al.* 2017a, b, Li *et al.* 2017). The static pre-stresses are applied by the axial compression system and limited to 200 MPa. The coal specimen is pre-stressed with 5 MPa static loads by an axial compression system referring to the surrounding coal stress state of roadway.

The stress-strain curves of coal specimens with different average water contents  $w_a$  are shown in Fig. 8. To avoid discreteness and minimize the errors in dynamic mechanical property experiments, three specimens with approximately equal water content were tested. Compared with static compressive tests, the specimens enter the elastic stage without a compaction stage, which makes the pre-peak region of the stress-strain curve nearly linear. The elastic modulus of coal specimen under dynamic load is larger than that of coal specimen under static load, and the dynamic compressive strength of the coal is greater than the static compressive strength for the coal specimen with roughly same water content.

The dynamic mechanical parameters of the coal specimens with the different water contents are shown in Fig. 9 and Table.

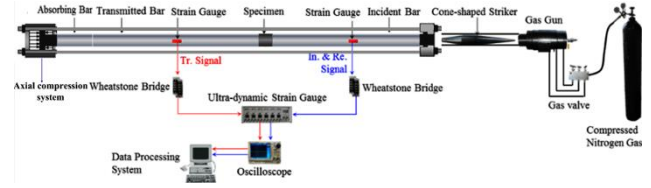


Fig. 7 Configuration of the SHPB system of coupled static-dynamic loads

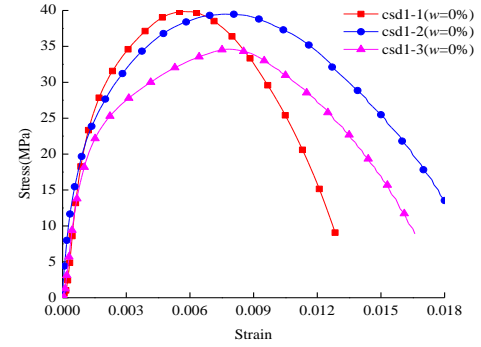
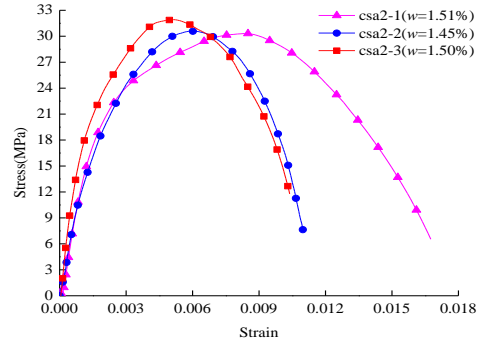
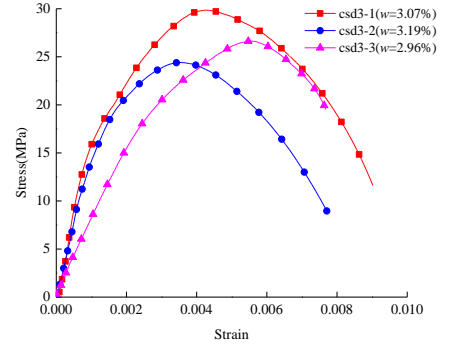
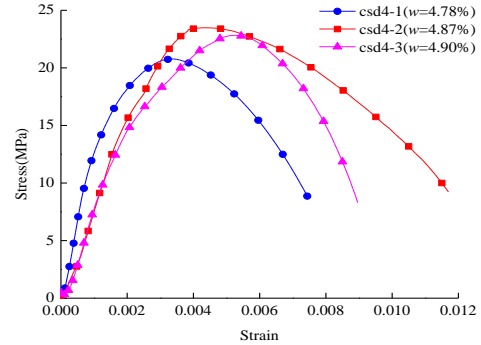

 (a)  $w_a=0\%$ 

 (b)  $w_a=1.49\%$ 

 (c)  $w_a=3.07\%$ 

 (d)  $w_a=4.85\%$ 

Fig. 8 Dynamic stress-strain curves of coal specimen with different average water contents

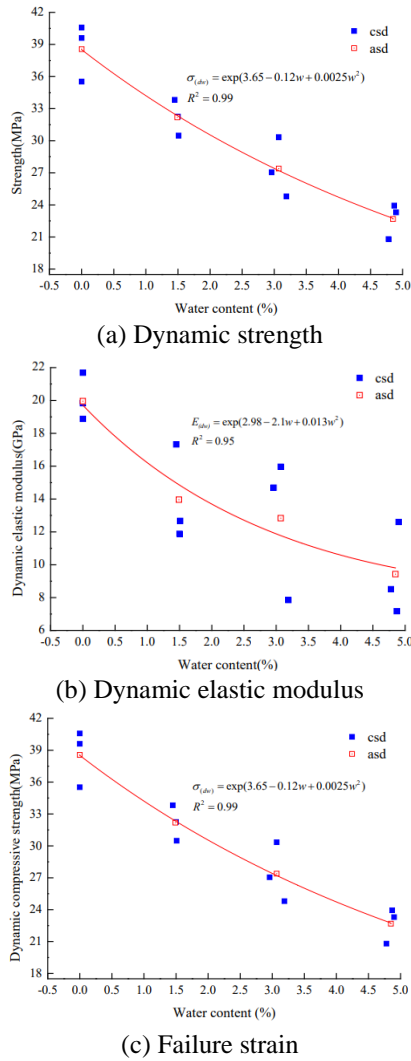


Fig. 9 Relation between dynamic mechanical parameters and water content (\*asd represents the mean value of dynamic mechanical parameters of specimens with the similar water content)

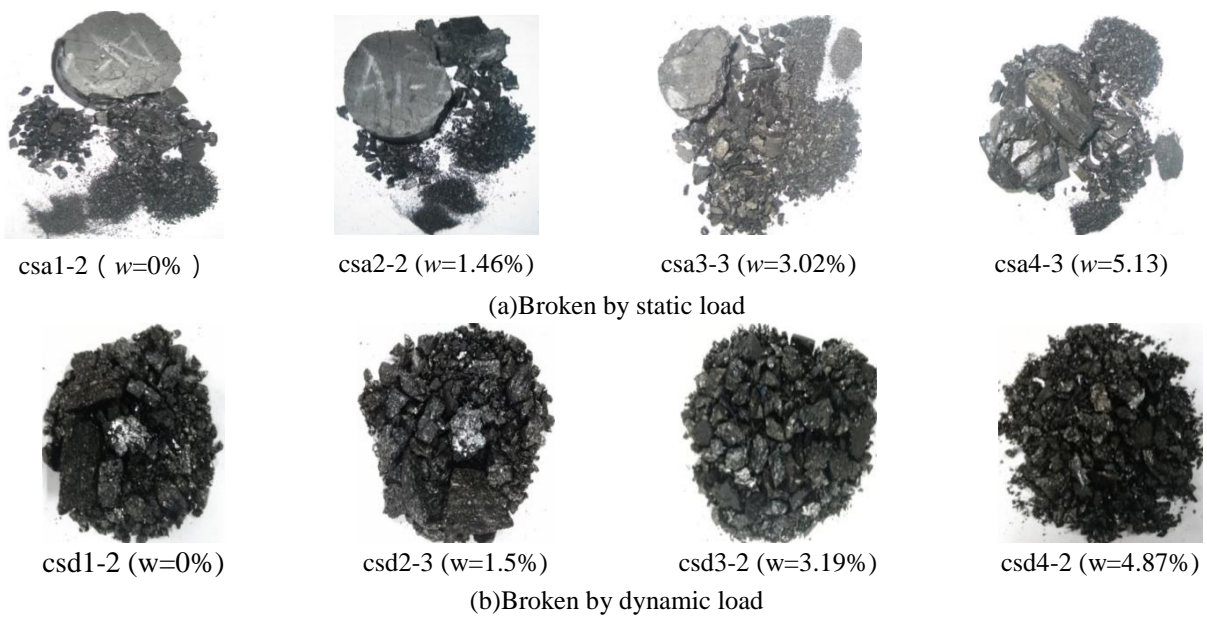


Fig. 10 Broken state of specimens with different water content under static and dynamic loads

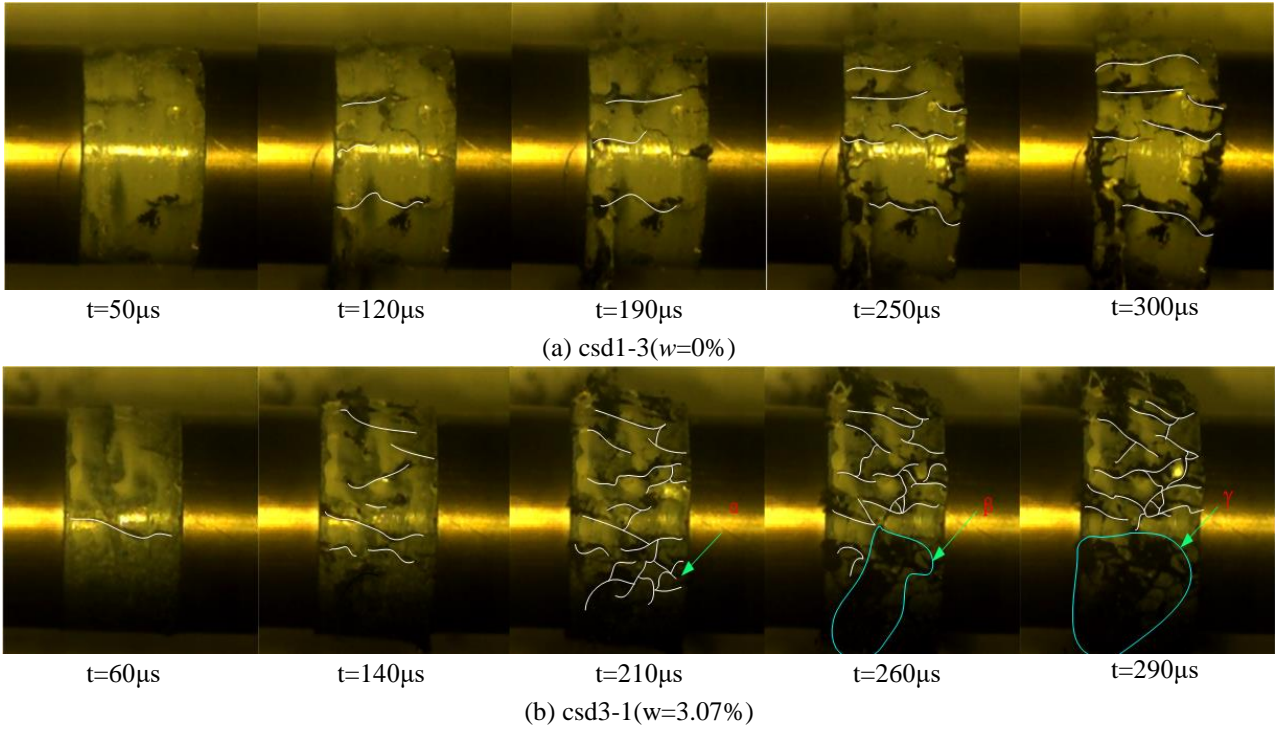


Fig. 11 Fracture development process of coal specimen under dynamic load

With increased water content, the dynamic compressive strength, elastic modulus and failure strain exponentially decline. The maximum reduction coefficient of the coal specimens, compared with their dry state, was approximately 48.7%, 66.9% and 63.8%, which manifest that water content has a significant influence on the dynamic mechanical properties of a coal specimen. At the peak, the dynamic compressive strength, elastic modulus and failure strain of coal specimens with lower water contents decrease more rapidly than these of the coal specimens with higher water contents. The regression analysis also reveals that the relations among the dynamic compressive strength, failure strain, dynamic elastic modulus and water content can be described by the equations in Table 3.

Fracture propagation and aggregation are the fundamental reason for the failure of coal specimen under dynamic loading (Xie *et al.* 2017, Fei *et al.* 2017). To explore the influence mechanism of water content on the fracture propagation of coal specimen, a high-speed camera (FASTCAM SA 1.1) is used for synchronously recording the fracture development process of coal specimens with two different water contents. The framing rate is set as 100,000fps. To better illustrate the development of fracture and failure process of specimens, take csd3-1 ( $w=3.07\%$ ) and csd1-3 ( $w=0\%$ ) as examples.

Fig. 11(a) shows that during dynamic load, the fractures are generated in the middle part on the left end of csd1-3, and expands gradually from the left end to the right end. It is worthy note that the expansion of all the fracture expands roughly along the direction of dynamic load until the specimen is destroyed. Fig. 11(b) shows the fracture development process of the coal specimen with the water

content of 3.07%. During dynamic impact, a serious of fractures with different lengths is generated on the specimen. And the fractures expand and prolonged with the increase of dynamic loading time. For csd3-1, when time at 210 $\mu$ s, a “bifurcation” phenomenon emerges from the branch fractured wall of the fracture, when the small fracture begins to appear and expand. Then, the width and length of the fracture in the fractured wall increase with the high rate, and the fracture density of the coal specimen with the water content of 3.07% is higher than that of the coal specimen with water content of 0%. In this case, the participation of water promotes the formation and expansion of fractures, thereby reducing the overall dynamic compressive strength and resistance to deformation of coal specimens.

## 5. Energy transmission and dissipation

Coal seam water infusion can change both of the dynamic mechanical characteristics and the stress wave propagation of the coal specimen. To explore the energy transmission and dissipation characteristics of stress wave, the stress waves of the coal specimen with different water contents were recorded by strain gauges on the incident bar and transmitted bar of SHPB, as shown in Fig. 12.

In the process of energy transmission and dissipation of coal with different water contents, the formulas used by Li and Gu (1994) were applied to calculate relate energy parameters of coal. And the dissipated energy of the coal specimen under dynamic load can be calculated as follows

$$E_c = E_i - E_r - E_t \quad (5)$$

where  $E_c$  is the dissipated energy of the coal specimen,  $E_I$ ,  $E_R$ , and  $E_T$  are energy carried by the incident, reflected, and transmitted wave, respectively, which are calculated as follows

$$E_I = \frac{A_e}{\rho_e C_e} \int_0^t \sigma_I^2(t) dt \quad (6)$$

$$E_R = \frac{A_e}{\rho_e C_e} \int_0^t \sigma_R^2(t) dt \quad (7)$$

$$E_T = \frac{A_e}{\rho_e C_e} \int_0^t \sigma_T^2(t) dt \quad (8)$$

where  $t$  is the duration of the stress wave,  $\rho_e c_e$  is the wave impedance of the bars,  $A_e$  is the cross-sectional area of the bars,  $\sigma_{(t)}$  denotes stress in the bar at time  $t$ , and the subscripts  $I$ ,  $R$ , and  $T$  refer to the incident, reflected and transmitted waves, respectively.

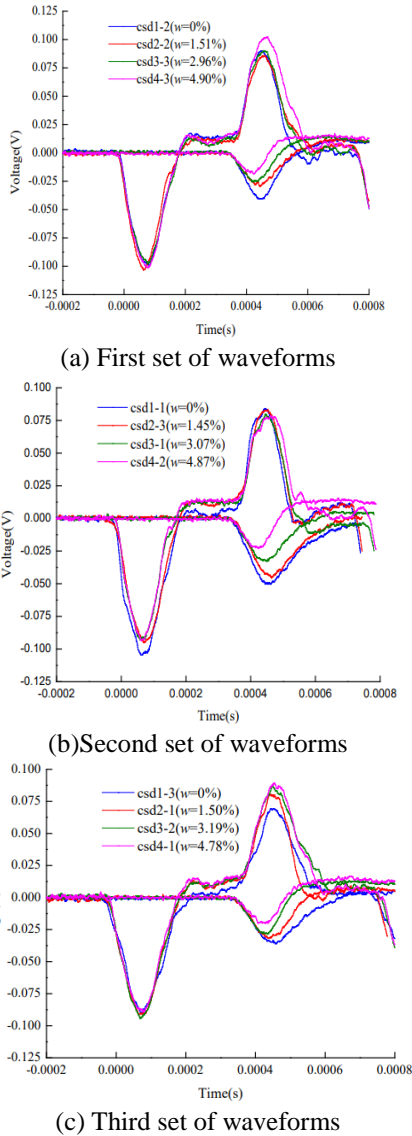


Fig. 12 Extracted signals in a typical dynamic compressive test

However, in the process, there is no participation of static load. For coal specimens under coupled static-dynamic loads, the static load makes the coal specimens store much of the elastic energy. The static compressive strength of coal specimen decline due to the influence of water content, and higher ratio of the stored elastic energy to the total energy are required for coal specimen failure. The influence of the stored energy on the dynamic energy release of the coal specimen during impact becomes greater. Therefore, it is necessary to consider the storage of the elastic energy of coal specimens under pre-stressed. The static deformation energy density  $w_s$  of the coal specimen under the static load can be expressed as follows

$$w_s = \int \sigma_i d\varepsilon_i \quad (9)$$

where  $\sigma_i$  is the axial static load stress at a certain point, and  $d\varepsilon_i$  is the deformation of the coal specimen under the axial static load. Thus, the deformation energy  $E_s$  can be expressed as follows

$$E_s = V_s w_s \quad (10)$$

where  $V_s$  is the volume of the coal specimen. During the dynamic test, the kinetic energy of the fragments produced by the failure of the coal specimen is much less (Zhang *et al.* 2000) and is ignored in this study. Thus, the calculation formula of dissipate energy can be expressed as follows

$$\begin{aligned} E_D &= V_s w_s + E_I - E_R - E_T \\ &= V_s \int \sigma_i d\varepsilon_i + \frac{A_e}{\rho_e C_e} \int_0^t \sigma_I^2(t) dt - \frac{A_e}{\rho_e C_e} \int_0^t \sigma_R^2(t) dt \\ &\quad - \frac{A_e}{\rho_e C_e} \int_0^t \sigma_T^2(t) dt \end{aligned} \quad (11)$$

where  $E_D$  is the dissipate energy of the coal under a coupled static-dynamic load. And the energy dissipation density can be expressed as follows

$$\kappa = E_D / V_s \quad (12)$$

Fig. 12 shows that under almost equal incident waves, the transmission and reflection waves of the coal specimen vary with the different water contents. To detail this rule and eliminate the influence of the incident wave on energy propagation, this paper uses the energy ratio to characterize it, which can be expressed as follows (Li and Gu 1994)

$$\text{Energy ratio: } \begin{cases} \text{TR} = \frac{E_T}{E_I} \\ \text{FR} = \frac{E_R}{E_I} \\ \text{DR} = \frac{E_D}{E_I} \end{cases}$$

where TR, FR and DR are energy transmittance rate, energy reflectivity rate and energy dissipation rate, respectively.

Fig. 13 shows that the energy transmittance rate and energy dissipation rate are decrease, while the energy reflectivity rate is increase slightly with increased water content. Meanwhile, the strength of coal decrease, and the

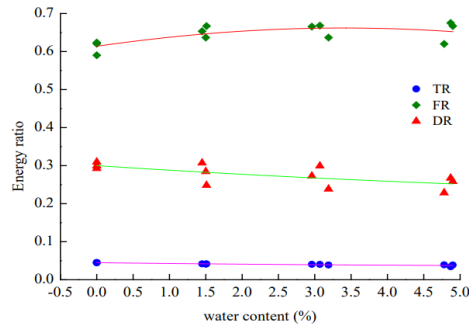


Fig. 13 Energy transfer characteristics of the stress wave in coal specimen with different water contents

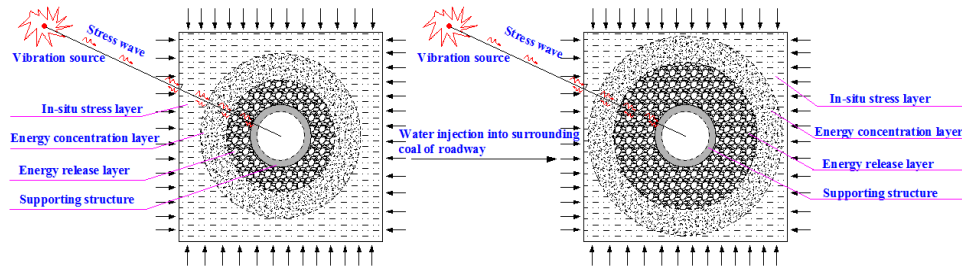


Fig. 14 Model of coal roadway before and after water infusion under dynamic load disturbance

coal specimen become more and more “softer”. The coal specimen between the incident bar and transmission bar plays a gradually strengthening role of “buffer cushion”, which lead to the gradual reduction of the energy dissipation and transfer capacity for coal specimen with increased water content.

For efficient coal burst prevention, the mechanism of coal seams water infusion preventing coal burst needs to be revealed from the dynamic mechanics perspectives (Ouyang *et al.* 2018). In the process of coal seam water infusion, water content of the coal will gradually increase. It will reduce the strength of coal and drive the high stress and concentrated elastic energy transfer to the deep part of the surrounding coal and form the new stress increase and elastic energy accumulate layer in deep part of surrounding coal. Meanwhile, the weak structural layer, i.e., energy release layer, expand on the basis of the original width and the layer plays as the role of “soft cushion”, that is, wave absorbing and energy absorbing, as shown in Fig. 14. From the experimental results can be known that the reflection energy is strengthened at the junction of high strength coal and the low strength coal with the water content increase in energy release layer. In the gradually increase process of the energy release layer width, the dissipation energy and the propagation ability of stress wave of the energy release layer are reduced, which manifests that water infusion can not only improve the stress environment of surrounding coal and inhibit coal burst in roadway surrounding coal.

The whole process of fracture initiation, propagation and instability failure of coal specimens during dynamic load are inevitably related to the energy dissipation and accompanied by the change strength (Peng *et al.* 2015), which is also a water content dependent procedure. Therefore, the strength characteristics of the coal specimen with different water contents under the dynamic load should be better interpreted with the concept of energy dissipation

(Ming *et al.* 2014). This study uses the conventional method, i.e., energy dissipation density instead of energy dissipation, to describe its relation with the dynamic compressive strength.

The abrupt release of energy will result in the failure of rock (Du *et al.* 2016). From Figs. 10 and 13, we can conclude that the magnitude of breakage is getting higher with increased water content under static and coupled static-dynamic loads, which indicate that water content can promote the destruction of coal specimen and reduce the per unit volume energy required for the failure of coal specimen. Energy dissipation density and failure magnitude of rock is closely related (Lundbrg 1976, Luo *et al.* 2017), and the failure magnitude is commonly characterized by lumpiness and fractal dimension (Turcotte 2002, Xie *et al.* 2003) after impact. These studies on the characteristics of energy dissipation and failure of rock are crucial to the dynamic failure mechanism of rock.

Fig. 15 gives the relationship between dynamic compressive strength and energy dissipation density of coal specimen with different water contents and the detail, as shown in Table 4. With the increase of energy dissipation density, the strength of coal specimen increases. This trend is not indifferent for coal specimens with different water contents, which can be described as: the smaller the water content, the more obvious the raise trend. And with the increase of water content, the slope of fitting curve decrease in sequence, which reflects that the dynamic compressive strength of coal specimen is not only controlled by the energy dissipation density, but also restricted by the water content.

Fig. 10(b) shows the failure state of coal specimens under different water contents, which indicates that the higher the water content, the more fragments that coal generates after dynamic load. For quantify describing the fragmentation of coal specimen, this analysis uses the

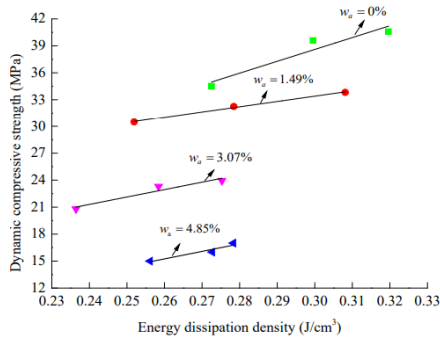


Fig. 15 The relation between dynamic compressive strength and energy dissipation density under different water contents

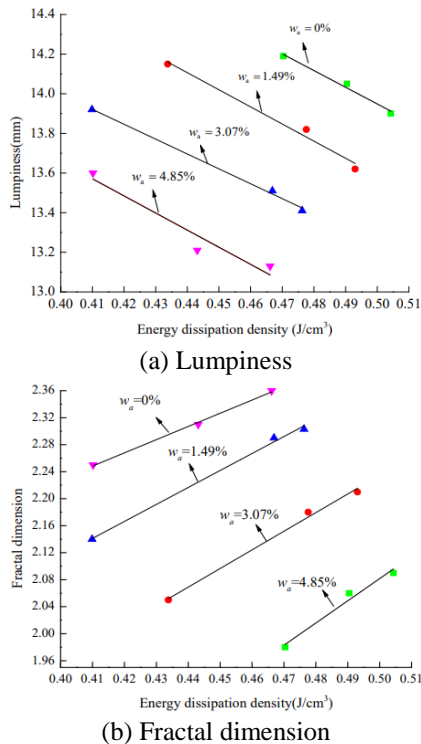


Fig. 16 The relation of failure characteristics and energy dissipation density under different water contents

method applied by Liu (2015) to measure the lumpiness of coal specimen after dynamic impact.

The lumpiness of coal specimens are calculated according to the collected fragments, as shown in Table 4. The relation of the lumpiness and the corresponding energy dissipation density of coal specimen is shown in Fig. 16(a), which illustrates that lumpiness decreases linearly with the increase of dissipation energy density under the approximately the same water content. Besides, the conclusions also indicate that the higher the water content, the smaller the lumpiness under the same energy dissipation density. It illustrates that water content can reduce the energy required for the expansion of the fracture under dynamic load and promote the crushing of the coal.

Furthermore, This study describe the fractal dimension of coal specimens after destruction, and obtain the relation of fractal dimension of coal specimen with different water contents and the energy dissipation density, as shown in Fig.

16(b).

The results of calculation are that the fractal dimension ranges of coal specimen with average water content  $w_a=0\%$ ,  $w_a=1.49\%$ ,  $w_a=3.07\%$  and  $w_a=4.85\%$  are 1.98~2.09, 2.05~2.21, 2.14~2.30 and 2.25~2.36, the specific results are shown in Table 4.

Fig. 16(b) shows that the fractal dimensions of the coal specimen with different water content increase with the increased energy dissipation density, which is generally opposite to that of lumpiness. It indicates that the irregularity of coal specimen damage can be promoted by water content and energy dissipation density.

## 6. Conclusions

In this study, the coal specimens with different water contents were tested by a series of laboratory tests, including XRD analysis, static load uniaxial compression test, and SHPB test to investigate the effects of water content on the static and dynamic mechanical properties of coal. The mechanisms of water content weakening coal specimen were discussed by analyzing the fracture propagation process of typical coal specimens. Meanwhile, the energy transmission and dissipation characteristics of the stress wave in coal specimens with different water contents and their effect on the failure features were further studied. The main conclusions as follows:

- The dynamic compressive strength, elastic modulus, and failure strain of coal specimens gradually decrease with the increase of water content.
- The participation of water promotes the expansion of fractures, and leading to the lumpiness of the coal specimens decreases with the increase of water content.
- The energy transmittance rate and energy dissipation rate are decrease, while the energy reflectivity rate is increase slightly with increased water content. The dynamic interpretation of water infusion preventing coal burst based on water infusion model of coal seam roadway under coupled static-dynamic loads was provided.
- The energy dissipation density of coal specimens is positively correlated with its dynamic compressive strength and lumpiness, and negative related to its fractal dimension. However, these parameters are negative correlated with the water content.

## Acknowledgements

The research presented in this paper was supported by the National Natural Science Foundation of China (Grant No.11772357, 41630642).

## References

- Cheng, J., Wan, Z., Zhang, Y., Li, W., Peng, S.S. and Zhang, P. (2015), "Experimental study on anisotropic strength and deformation behavior of a coal measure shale under room dried and water saturated conditions", *Shock Vib.*, 1-13.
- Cheng, W. M., Nie, W., Zhou, G., Yu, Y., Ma, Y. and Xue, J.

- (2012), "Research and practice on fluctuation water infusion technology at low permeability coal seam", *Safety Sci.*, **50**(4), 851-856.
- Du, K., Tao, M., Li, X.B. and Zhou, J. (2016), "Experimental study of slabbing and rockburst induced by true-triaxial unloading and local dynamic disturbance", *Rock Mech. Rock Eng.*, **49**(9), 1-17.
- Fei, H.L. and Hong, C.C. (2017), "Study on crushed and fracture zone range under combined action of stress and detonation gas", *Blasting*, **34**(1), 33-36 (in Chinese).
- Gaziev, E. (2001), "Rupture energy evaluation for brittle materials", *J. Solid. Struct.*, **38**(42), 7681-7690.
- Hong, L., Zhou, Z.L., Yin, T.B., Liao, G.Y. and Ye, Z.Y. (2009), "Energy consumption in rock fragmentation at intermediate strain rate", *J. Central South Univ. Technol.*, **16**(4), 677-682.
- ISRM. (1978), "Suggested methods for determining tensile strength of rock materials", *J. Rock Mech. Min. Sci. Geomech. Abstr.*, **15**(15), 99-103.
- Li, M., Mao, X., Lu, A., Tao, J., Zhang, G., Zhang, L. and Li, C. (2014), "Effect of specimen size on energy dissipation characteristics of red sandstone under high strain rate", *J. Min. Sci. Technol.*, **24**(2), 151-156.
- Li, X. and Gu, D. (1994), *Rock Impact Dynamics*, Central South University of Technology Press, Changsha, China.
- Li, X., Tao, M., Wu, C., Du, K. and Wu, Q. (2017), "Spalling strength of rock under different static pre-confining pressures", *J. Impact Eng.*, **99**, 69-74.
- Li, X., Zhou, Z., Lok, T. S., Hong, L. and Yin, T. (2008), "Innovative testing technique of rock subjected to coupled static and dynamic loads", *J. Rock Mech. Min. Sci.*, **45**(5), 739-748.
- Li, X., Zou, Y. and Zhou, Z. (2014), "Numerical simulation of the rock shpb test with a special shape striker based on the discrete element method", *Rock Mech. Rock Eng.*, **47**(5), 1693-1709.
- Liu, J., Xu, J., Lu, X., Zhang, L. and Wang, Z. (2009), "Experimental study on dynamic mechanical properties of amphibolites under impact compressive loading", *Chin. J. Rock Mech. Eng.*, **28**(10), 2113-2120.
- Liu, X., Dai, F., Zhang, R. and Liu, J. (2015), "Static and dynamic uniaxial compression tests on coal rock considering the bedding directivity", *Environ. Earth Sci.*, **73**(10), 5933-5949.
- Lundberg, B. (1976), "A split hopkinson bar study of energy absorption in dynamic rock fragmentation", *J. Rock Mech. Min. Sci. Geomech. Abstr.*, **13**(6), 187-197.
- Luo, X.L., Mo, J.Y., Chi, E.A. and Li, Y.N. (2017), "Experimental study and optimization of blasting parameters of high water cut rock", *Blasting*, **34**(4), 85-90 (in Chinese).
- Ogata, Y., Jung, W., Kubota, S. and Wada, Y. (2004), "Effect of the strain rate and water saturation for the dynamic tensile strength of rocks", *Mater. Sci. Forum*, **465-466**, 361-366.
- Ouyang, Q., Wu, C. and Huang, L. (2018), "Methodologies, principles and prospects of applying big data in safety science research", *Safety Sci.*, **101**, 60-71.
- Peng, R., Ju, Y., Wang, J.G., Xie, H., Gao, F. and Mao, L. (2015), "Energy dissipation and release during coal failure under conventional triaxial compression", *Rock Mech. Rock Eng.*, **48**(2), 509-526.
- Shen, J., Jimenez, R., Karakus, M. and Xu, C. (2014), "A simplified failure criterion for intact rocks based on rock type and uniaxial compressive strength", *Rock Mech. Rock Eng.*, **47**(2), 357-369.
- Shen, J., Karakus, M. and Xu, C. (2012), "A comparative study for empirical equations in estimating deformation modulus of rock masses", *Tunn. Undergr. Sp. Technol.*, **32**(11), 245-250.
- Tao, M., Ma, A., Cao, W., Li, X. and Gong, F. (2017b), "Dynamic response of pre-stressed rock with a circular cavity subject to transient loading", *J. Rock Mech. Min. Sci.*, **99**, 1-8.
- Tao, M., Zhao, H., Li, X., Ma, J., Du, K. and Xie, X. (2017a), "Determination of spalling strength of rock by incident waveform", *Geomech. Eng.*, **12**(1), 1-8.
- Turcotte, D.L. (2002), "Fractals in petrology", *Lithos*, **65**(3-4), 261-271.
- Whittles, D.N., Kingman, S., Lowndes, I. and Jackson, K. (2006), "Laboratory and numerical investigation into the characteristics of rock fragmentation", *Mineral. Eng.*, **19**(14), 1418-1429.
- Xie, G., Yin, Z., Wang, L., Hu, Z. and Zhu, C. (2017), "Effects of gas pressure on the failure characteristics of coal", *Rock Mech. Rock Eng.*, **50**(1), 1-13.
- Xie, H., Gao, F. and Zhou, H. (2003), "Fractal fracture and fragmentation in rocks", *J. Seismol.*, **23**(4), 1-9.
- Yao, Q., Li, X., Zhou, J., Ju, M., Chong, Z. and Zhao, B. (2015), "Experimental study of strength characteristics of coal specimens after water intrusion", *Arab. J. Geosci.*, **8**(9), 6779-6789.
- Zhang, Z.X., Kou, S.Q., Jiang, L.G. and Lindqvist, P.A. (2000), "Effects of loading rate on rock fracture: Fracture characteristics and energy partitioning", *J. Rock Mech. Min. Sci.*, **37**(5), 745-762.
- Zhao, Y., Liu, S., Jiang, Y., Wang, K. and Huang, Y. (2016), "Dynamic tensile strength of coal under dry and saturated conditions", *Rock Mech. Rock Eng.*, **49**(5), 1709-1720.
- Zheng, Z., Khodaverdian, M. and McLennan, J.D. (1991), "Static and dynamic testing of coal specimens", *Proceedings of the 1991 SCA Conference*, San Antonio, Texas, U.S.A.
- Zhou, Y.X., Xia, K.W., Li, X.B., Li, H.B., Ma, G.W., Zhao, J., Zhou, Z.L. and Dai, F. (2011), "Suggested methods for determining the dynamic strength parameters and mode-I fracture toughness of rock materials", *J. Rock Mech. Min. Sci.*, **49**(1), 105-112.
- Zhou, Z., Cai, X., Cao, W., Li, X. and Xiong, C. (2016), "Influence of water content on mechanical properties of rock in both saturation and drying processes", *Rock Mech. Rock Eng.*, **49**(8), 3009-3025.
- Zhou, Z., Li, X., Liu, A. and Zou, Y. (2011), "Stress uniformity of split hopkinson pressure bar under half-sine wave loads", *J. Rock Mech. Min. Sci.*, **48**(4), 697-701.

CC